
PHASE
TRANSITIONS

Structural Instability in BaZrO₃ Crystals: Calculations and Experiment

A. I. Lebedev* and I. A. Sluchinskaya

Moscow State University, Moscow, 119991 Russia

* e-mail: swan@scon155.phys.msu.ru

Received March 4, 2013

Abstract—The phonon spectrum of cubic barium zirconate is calculated from first principles using the density functional theory. An unstable R_{25} phonon mode observed in the phonon spectrum indicates an instability of the BaZrO₃ structure with respect to the oxygen octahedra rotations. It is shown that the symmetry of the ground-state structure of the crystal is $I4/mcm$. The local structure of BaZrO₃ is studied by the EXAFS spectroscopy at the BaL_{III} absorption edge at 300 K to search for the instability predicted by calculations. Anomalous high values of the Debye–Waller factor for the Ba–O atomic pairs ($\sigma_1^2 \sim 0.015 \text{ \AA}^2$) are attributed to the appearance of this structural instability. The average amplitude of the octahedra rotations caused by thermal vibrations is estimated from the measured σ_1^2 value to be $\sim 4^\circ$ at 300 K. The closeness of the calculated energies of various distorted phases resulting from the condensation of the R_{25} mode suggests a possible formation of the structural glass state in BaZrO₃ as the temperature is lowered. It explains the origin of the disagreement between the results of calculations and diffraction experiments.

DOI: 10.1134/S1063783413090229

1. INTRODUCTION

Crystals of the perovskite family are widely used in modern technology and applications. This is due to the lability of their crystal structure which allows them to undergo various (ferroelectric, ferroelastic, magnetic, and superconducting) phase transitions.

Barium zirconate BaZrO₃ having the perovskite structure is widely used in microwave electronics. Its solid solutions with BaTiO₃ are relaxors with a very high electric-field tuning of the dielectric constant and are promising for applications in tunable filters, generators, phase shifters, and phased array antennas [1, 2]. When doped with yttrium, BaZrO₃ becomes an ionic conductor with high proton conductivity promising for applications in fuel cells [3].

According to X-ray and neutron diffraction studies, barium zirconate retains its cubic structure up to the lowest temperatures (2 K) [4] and exhibits no phase transitions. However, these structural data disagree with the results of the first-principles calculations of the BaZrO₃ phonon spectrum (see [4–7] and also [8]), which reveal an instability of the R_{25} mode in the phonon spectrum and predict an instability of the BaZrO₃ cubic structure with respect to the octahedra rotations. An indirect evidence of the possible phase transformation in BaZrO₃ can be its very low thermal expansion coefficient at temperatures below 300 K [4]. It was supposed that the disagreement between theory and experiment is caused by the fact that the long-

range order in the octahedra rotations is not established for some reasons in these crystals even at low temperatures. In particular, in [6] it was suggested that zero-point lattice vibrations can be such a reason.

The aim of this work was to calculate the phonon spectrum and the ground-state structure of BaZrO₃ from first principles and to find experimental evidences for the structural instability in these crystals. Our idea was that even if the long-range order in this material is absent for some reason, the structural instability (if it exists) should manifest itself in a change of the *local* structure. To search for such changes, we used the extended X-ray absorption fine structure technique (EXAFS spectroscopy). This is one of the powerful modern experimental techniques which provides a detailed information primarily on the local crystal structure [9]. We expected to obtain evidences of the BaZrO₃ structural instability from an anomalous behavior of Debye–Waller factors which characterize the local displacements and amplitude of thermal vibrations.

2. CALCULATION TECHNIQUE AND RESULTS

The calculations were performed from first principles within the density functional theory using the ABINIT program. Pseudopotentials for Ba, Zr, and O atoms were borrowed from [10, 11]. The maximum energy of plane waves in the calculations was 30 Ha

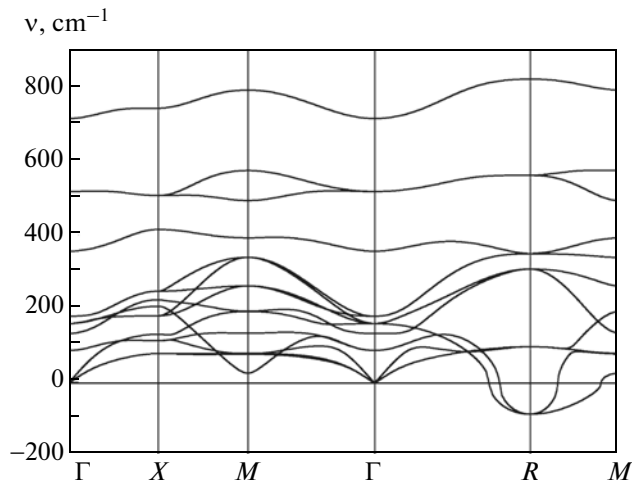


Fig. 1. Phonon spectrum of BaZrO₃ in the cubic *Pm3m* phase.

(Hartree) (816 eV). Integration over the Brillouin zone was performed on the $8 \times 8 \times 8$ Monkhorst–Pack mesh. The lattice parameters and equilibrium positions of atoms were calculated from the condition of a decrease of the Hellmann–Feynman forces below 5×10^{-6} Ha/Bohr (0.25 meV/Å) while the total energy calculation accuracy was better than 10^{-10} Ha. The phonon spectra were calculated using the formulas derived in the perturbation theory and the interpolation technique described in [10]. The calculated lattice parameter for cubic BaZrO₃ (4.1659 Å) is in good agreement with the experimental value obtained at 10 K (4.191 Å [4]). The minor disagreement of these values is caused by the systematic underestimation of the lattice parameter, typical of the local density approximation (LDA) used in this work.

The phonon spectrum of cubic BaZrO₃ with the perovskite structure (space group *Pm3m*) is shown in Fig. 1. An unstable phonon of the R_{25} symmetry presenting in this spectrum (the imaginary values of the phonon energy are given by negative numbers in the figure) suggests that the cubic structure is unstable with respect to the octahedra rotations. The results of these calculations agree with the results of previous studies [4–8]; however, it should be noted that an

Table 1. Energy of various distorted BaZrO₃ structures (the energy of the cubic *Pm3m* phase is taken as the energy reference point)

Unstable mode	Glazer rotations	Space group	Energy, meV
R_{25}	$a^-a^-a^-$	$R3c$	−9.17
R_{25}	$a^0b^-b^-$	$Imma$	−9.47
R_{25}	$a^0a^0c^-$	$I4/mcm$	−10.01

additional instability at the *M* point found in [6] was not observed in our calculations.

To determine the ground-state structure, we calculated the energies of various distorted phases which can arise from the cubic perovskite structure as a result of condensation of the unstable triply degenerate R_{25} mode, taking into account its degeneracy. If we write the expansion of the total energy of a crystal in a power series of the distortion amplitudes in the spirit of the Landau expansion,

$$\begin{aligned}
 E_{\text{tot}} = & E_{\text{tot}}(0) + a(\phi_x^2 + \phi_y^2 + \phi_z^2) \\
 & + b(\phi_x^2 + \phi_y^2 + \phi_z^2)^2 + c(\phi_x^4 + \phi_y^4 + \phi_z^4) \\
 & + d(\phi_x^2 + \phi_y^2 + \phi_z^2)^3 + e\phi_x^2\phi_y^2\phi_z^2 + \dots,
 \end{aligned} \quad (1)$$

where $E_{\text{tot}}(0)$ is the total energy of the cubic phase, ϕ_x , ϕ_y , and ϕ_z are the rotation angles about three fourfold axes, it becomes evident that, to search for the ground state, it is sufficient to calculate the energies of the phases described by the order parameters $(\phi, 0, 0)$, $(\phi, \phi, 0)$, and (ϕ, ϕ, ϕ) at which the E_{tot} minimum is reached for various combinations of signs of the expansion coefficients c and e . These order parameters correspond to the Glazer rotation systems ($a^0a^0c^-$), ($a^0b^-b^-$), and ($a^-a^-a^-$) and result in space groups $I4/mcm$, $Imma$, and $R\bar{3}c$, respectively. As follows from Table 1, the $I4/mcm$ phase has the lowest energy among these phases. This phase appears from the *Pm3m* cubic structure by out-of-phase octahedra rotations about one of the fourfold axes. The energy of this phase is lower than the energy of the cubic phase by ~ 10 meV, which corresponds to an approximate phase transition temperature of ~ 120 K.

It should be noted that among the obtained solutions there is no $P\bar{1}$ phase which was considered as the ground state in [5]. This phase corresponds to the Glazer rotation system ($a^-b^-c^-$) in which the rotation angles about three fourfold axes of the cubic structure are different. A check of this solution showed that the $P\bar{1}$ structure slowly relaxes to the above $I4/mcm$ solution; however, the convergence required more than 400 iterations. This shows that the use of information about the crystal symmetry in the calculation of the total energy makes it possible to significantly (more than tenfold) reduce the calculation time needed to search for the ground-state structure and guarantees accurate results.

The lattice parameters and atomic coordinates in the ground-state structure of barium zirconate are given in Table 2.

Table 2. Calculated lattice parameters and atomic coordinates in the BaZrO₃ ground-state structure

Phase	Lattice parameters, Å	Atom	Position	<i>x</i>	<i>y</i>	<i>z</i>
<i>I4/mcm</i>	<i>a</i> = 5.8722 <i>c</i> = 8.3577	Ba	4 <i>b</i>	0	0.50000	0.25000
		Zr	4 <i>c</i>	0	0	0
		O	4 <i>a</i>	0	0	0.25000
		O	8 <i>h</i>	0.22315	0.72315	0

Table 3. Structural parameters for the first three shells in cubic BaZrO₃ at 300 K obtained from EXAFS data analysis

Measurement technique	<i>R</i> ₁ , Å	σ_1^2 , Å	<i>R</i> ₂ , Å	σ_2^2 , Å	<i>R</i> ₃ , Å	σ_3^2 , Å
Fluorescence	2.916	0.0155	3.640	0.0079	4.244	0.0101
Transmission	2.914	0.0145	3.635	0.0068	4.244	0.0087

3. SAMPLES AND EXPERIMENTAL TECHNIQUE

The samples of barium zirconate were prepared by the solid-state reaction method. The starting components were BaCO₃ and microcrystalline ZrO₂ obtained by the decomposition of ZrOCl₂ · 8H₂O at 300°C. Components were dried at 600°C, weighted in appropriate proportions, ground in acetone, and annealed in air at 1100°C for 6 h. The prepared powders were ground again and repeatedly annealed at a temperature of 1500°C for 3 h. The single-phase nature of the samples was confirmed by X-ray diffraction.

The EXAFS spectra were recorded by simultaneous measurement of the transmission and X-ray fluorescence at the KMC-2 station of the BESSY synchrotron radiation source (the beam energy is 1.7 GeV; the beam current is up to 300 mA) at the BaL_{III} edge (5.247 keV) at 300 K. The intensity of the radiation incident on the sample was measured using an ionization chamber; the intensity of the radiation passed through the sample was measured using a silicon photodiode, and the intensity of the fluorescence excited in the sample was measured using a RÖNTEC silicon energy-dispersive detector. A total of four spectra were recorded.

The BaL_{III} edge was chosen because the predicted structural instability accompanied by the oxygen octahedra rotations should most strongly manifest itself in the EXAFS measurements of the Ba–O interatomic distances, rather than of the Zr–O interatomic distances, since the latter remain almost unchanged when the octahedra are rotated. In principle, the octahedra rotations could also be observed in the changes of the multiple scattering contributions to the EXAFS spectra at the Zr *K* edge; this technique is described in [12].

The EXAFS spectra were independently processed in the conventional way [13]; the results obtained were then averaged. According to our theoretical evalua-

tions, the temperature of the expected phase transition is below 300 K; therefore, in the data analysis we considered the BaZrO₃ structure as cubic and assumed that the structural instability in it will manifest itself as overestimated Debye–Waller factors.

4. EXPERIMENTAL RESULTS AND DISCUSSION

The typical EXAFS spectrum of the BaZrO₃ sample recorded at the BaL_{III} edge at 300 K is shown in Fig. 2. The data analysis shows that the spectra are in good agreement with a model in which the structure of the samples under study is cubic. The structural parameters (interatomic distances *R*_{*i*} and Debye–

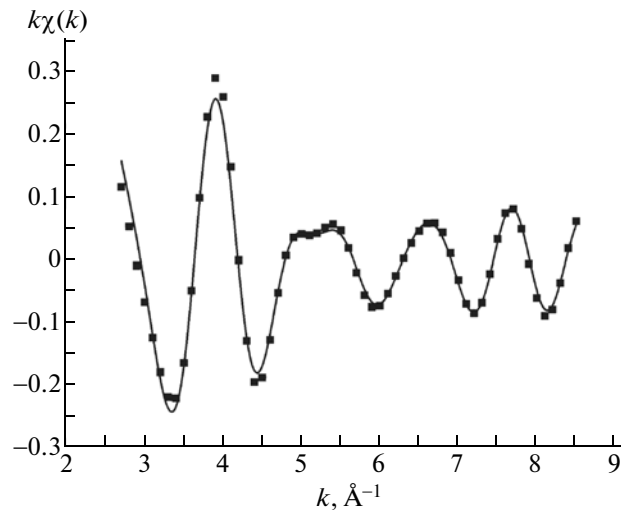


Fig. 2. Typical EXAFS spectrum of the BaZrO₃ sample obtained at the BaL_{III} edge at 300 K (squares) and the result of its fitting (solid curve). The limited wavenumber *k* range is caused by the closeness of the BaL_{III} and BaL_{II} absorption edges.

Waller factors σ_i^2) for the first three shells are given in Table 3. One can see that the structural parameters determined by two different measurement techniques (transmission and fluorescence) are almost identical.

In Table 3, attention should be drawn to an overestimated Debye–Waller factors for the first shell, which are significantly larger than those for the second and third shells (usually, this factor monotonically increases with increasing interatomic distance).

The Debye–Waller factor is usually controlled by two components: static distortion of the structure and thermal vibrations. Since our measurements are performed above the temperature of the expected phase transition, no static distortions should be observed. Further, the optical modes responsible for the ZrO_6 octahedron deformation are the highest-frequency ones in the BaZrO_3 phonon spectrum and are almost not excited at 300 K. Therefore, we can consider this octahedron as a rigid one. The thermal motion of the center of this octahedron with respect to the Ba atom is described by the Debye–Waller factor σ_2^2 . Since, by virtue of the octahedron rigidity, the oxygen atoms are strongly bound to Zr atoms, the only way to explain why $\sigma_1^2 \gg \sigma_2^2$ is to take into account the octahedra rotations. Assuming that the Debye–Waller factors for Ba–O and Ba–Zr bonds in the absence of the octahedra rotations are close (0.008 \AA^2), we can attribute the excess part $\Delta\sigma_1^2$ of the Debye–Waller factor in the first shell to the thermal rotational vibrations. Then, using the formula

$$\Delta\sigma_1^2 = \frac{a_0^2 \theta^2}{12}$$

which describes the dependence of $\Delta\sigma_1^2$ on the octahedra rotation angle θ about the fourfold axis of the cubic structure, we can estimate the amplitude of rotational vibrations. For the lattice parameter $a_0 \approx 4.2 \text{ \AA}$,

it is $\sqrt{\theta^2} \approx 4^\circ$. For comparison, in SrTiO_3 , in which the structural phase transition occurs at 105 K, the experimental oxygen octahedra rotation angle at 50 K is 2.01° [14] which is comparable to the amplitude of rotational vibrations in BaZrO_3 determined in our study.

We now discuss the causes of the absence of the long-range order in the octahedra rotations in BaZrO_3 at low temperatures. As noted in the Introduction, the suppression of the long-range order by zero-point lattice vibrations was considered as one of the causes of such behavior. In [15], a criterion was proposed which enables us to estimate the stability of a structure with respect to zero-point vibrations and is based on a set of parameters calculated completely from first principles. According to this criterion, zero-point vibrations

make the system localization in one of the local minima of the potential energy impossible at $h\nu/E_0 > 2.419$, where ν is the frequency of the unstable phonon and E_0 is the depth of the local minimum of the potential energy. For the unstable R_{25} mode in BaZrO_3 , $h\nu = 81.2 \text{ cm}^{-1} \approx 10 \text{ meV}$ and $E_0 \approx 10 \text{ meV}$ (Table 1); hence, zero-point vibrations should not suppress the structural distortions in barium zirconate. The fact that the influence of zero-point vibrations on the phase transition in BaZrO_3 is weaker than in SrTiO_3 is not surprising since the masses of both metal atoms in barium zirconate are larger. Thus, the explanation of the suppression of the long-range order in BaZrO_3 by zero-point vibrations proposed in [6] seems unlikely.

The theoretical calculations carried out in this work allow us to propose another explanation of the absence of the long-range order in BaZrO_3 exhibiting the structural instability. The closeness of the energies of the $R\bar{3}c$, $Imma$, and $I4/mcm$ phases (Table 1) which can emerge from the condensation of the R_{25} mode, on the one hand, and the fact that the transitions between these phases are of the first order, on the other hand, suggest that the structural glass state appears in the crystal upon cooling. Internal strains and defects in the samples result in the condensation of phases with different octahedral rotation patterns at different points of the sample, which obviously leads to the absence of the long-range order in their rotations. Furthermore, the oxygen vacancies, which are rather easily formed in BaZrO_3 , break the three-dimensional connectivity of the perovskite structure and, hence, promote the formation of the structural glass state. The uniqueness of barium zirconate among other crystals with the perovskite structure is that the energy difference between the phases with different rotation patterns is only 0.84 meV (Table 1), which is much smaller than that in other crystals we have studied (3.4 meV in SrTiO_3 , 136 meV in CaTiO_3 , 371 meV in CdTiO_3 [10, 15], and 69 meV in SrZrO_3). This explains the tendency of BaZrO_3 to the formation of the structural glass state.

5. CONCLUSIONS

The first-principles calculations of the BaZrO_3 phonon spectrum and the experimental observation of anomalously high Debye–Waller factors for the Ba–O bonds in EXAFS measurements suggest that the structural instability with respect to the oxygen octahedra rotations indeed exists in barium zirconate. It was shown that zero-point lattice vibrations are not the factor which prevents the formation of the long-range order in the octahedra rotations. The extreme closeness of the energies of phases with different octahedral rotation patterns which can result from the condensation of the R_{25} phonon in BaZrO_3 enables us to suggest the transition to the structural glass state upon cooling.

This explains the apparent contradiction between predictions of the calculations and the experimentally observed absence of the long-range order in the octahedra rotations. Further experimental studies of BaZrO₃, such as the study of the temperature dependence of diffraction line width, diffuse scattering, elastic properties, and other physical phenomena sensitive to the octahedra rotations could yield additional information about the causes of disagreement between theory and experiment and prove or disprove the hypothesis proposed in this work.

ACKNOWLEDGMENTS

The calculations presented in this work were performed on the laboratory computer cluster (16 cores). The authors are grateful to the BESSY staff for help in preparation of experiment and to the Russian–German laboratory for financial support during their stay at BESSY.

This work was partially supported by the Russian Foundation for Basic Research (project no. 13-02-00724).

REFERENCES

1. T. Maiti, R. Guo, and A. S. Bhalla, *Appl. Phys. Lett.* **90**, 182901 (2007).
2. Q. Zhang, J. Zhai, and L. B. Kong, *J. Adv. Dielectr.* **2**, 1230002 (2012).
3. K. Kreuer, *Annu. Rev. Mater. Res.* **33**, 333 (2003).
4. A. R. Akbarzadeh, I. Kornev, C. Malibert, L. Bellaiche, and J. M. Kiat, *Phys. Rev. B: Condens. Matter* **72**, 205104 (2005).
5. J. W. Bennett, I. Grinberg, and A. M. Rappe, *Phys. Rev. B: Condens. Matter* **73**, 180102(R) (2006).
6. A. Bilić and J. D. Gale, *Phys. Rev. B: Condens. Matter* **79**, 174107 (2009).
7. C. Zhu, K. Xia, G. R. Qian, C. L. Lu, W. Z. Luo, K. F. Wang, and J.-M. Liu, *J. Appl. Phys.* **105**, 044110 (2009).
8. W. Zhong and D. Vanderbilt, *Phys. Rev. Lett.* **74**, 2587 (1995).
9. P. A. Lee, P. H. Citrin, P. Eisenberger, and B. M. Kincaid, *Rev. Mod. Phys.* **53**, 769 (1981).
10. A. I. Lebedev, *Phys. Solid State* **51** (2), 362 (2009).
11. A. I. Lebedev, *Phys. Solid State* **52** (7), 1448 (2010).
12. B. Rechav, Y. Yacoby, E. A. Stern, J. J. Rehr, and M. Newville, *Phys. Rev. Lett.* **72**, 1352 (1994).
13. A. I. Lebedev, I. A. Sluchinskaya, V. N. Demin, and I. H. Munro, *Phys. Rev. B: Condens. Matter* **55**, 14770 (1997).
14. W. Jauch and A. Palmer, *Phys. Rev. B: Condens. Matter* **60**, 2961 (1999).
15. A. I. Lebedev, *Phys. Solid State* **51** (4), 802 (2009).

Translated by A. Kazantsev